On the occurrence of wave breaking

Johannes Gemmrich

University of Victoria, Victoria, BC, Canada

Abstract. The practicality of common wave breaking criteria is reviewed. Video recordings of the sea surface taken from aboard R/P FLIP are used to extract breaking wave properties. The key quantity is $\Lambda(c)dc$, the length of breaking crests per unit area propagating with speeds in the range (c, $c+dc$). Independent of wave field development, $\Lambda(c)$ is found to peak at intermediate wave scales and to drop off sharply at larger and smaller scales. For young waves, breakers occur at a wide range of scales corresponding to phase speeds of about 0.1-1.0 c_p, but in developed seas breaking is hardly observed at scales corresponding to phase speeds >0.5 c_p. The phase speed of the most frequent breakers shifts from 0.4 c_p to 0.2 c_p as the wave field develops. The relative distribution of breaker scale increases the likelihood of rogue waves in developed seas compared to young seas. The overall breaking rate correlates well with the fraction of steep waves.

Introduction

Regardless of a precise definition and an exact generation mechanism, rogue waves are seen as single large waves standing out of a wave record of suitable length of say several tens of minutes. Assuming the wave length of a rogue wave to be comparable to the dominant wave length implies rogue waves are therefore relatively steep waves. However, if their steepness exceeds a certain threshold one would expect a significant amount of wave breaking. Thus wave breaking and rogue waves are intimately related.

More generally, surface waves have been labeled as the gearbox between atmosphere and ocean (*Ardhuin et al.*, 2005) and wave breaking plays an important role in many air-sea exchange processes. Breaking waves not only transfer energy, momentum, heat, and gases from the atmosphere to the ocean surface layer but also enhance aerosol generation and latent heat fluxes due to sea spray. Breaking waves also disperse pollutants and generate underwater sound. Furthermore, wave breaking affects wave development as it dominates the dissipation of wave energy and controls wave growth.

To improve our understanding of wave-breaking related processes a twofold approach is necessary: i) detailed process studies, e.g., energy dissipation, mixing, sound generation, etc., and ii) knowledge of the occurrence and scale of wave breaking. Here I will focus on the latter and review wave breaking conditions in open ocean environments.

Wave breaking criteria

A central question to many wave related issues is: what are the conditions required for waves to break? So far, no answer has been found that is solid on theoretical grounds, can be verified by observations, and is easily incorporated into wave models.

There are three classes of direct wave breaking criteria: the kinematics, geometry, and dynamics of waves.

The *kinematic* criterion is the most fundamental definition of wave breaking, stating that the horizontal particle speed of the fluid at the crest exceeds the wave phase speed. For irrotational waves this leads to the *geometric* criterion that a wave at the point of breaking is a Stokes wave with a limiting crest angle of 120° and a maximum steepness $(ak)_{\max} = \pi/7$, where a and k are wave amplitude and wave number, respectively. From a *dynamical* point of view waves break when the Lagrangian downward acceleration $-\eta_{tt}$ of the fluid at the crest exceeds a portion of the gravitational acceleration g: $-\eta_{tt} > \alpha g$, where $\alpha = 0.5$ for the Stokes wave but $\alpha < 0.39$ for the so-called almost steepest waves (*Longuet-Higgins,* 1985).

Kinematic breaking criterion

It is impractical to directly measure fluid particle speeds within wave crests. Indirect methods relating particle speed to surface elevation are invalid in the case of rotational waves. Hence, the kinematic wave-breaking criterion is not applied to wave data.

Geometric breaking criterion

It would seem to be straightforward to monitor wave steepness. However, the steepness of individual waves cannot be defined uniquely in a broad band wave field. The challenge lies in defining an individual wave. Let us consider three different approaches to the analysis of a fixed point surface elevation time series $\eta(t)$.

(i) Zero-crossing analysis: A wave might be defined as the period T_{br} between two successive instances of $\eta_t = 0$, $\eta_{tt} > 0$, i.e. the period between two local wave troughs, and the wave height H_{br} which is defined as the difference between the surface elevations at the crest and the leading trough (Figure 1). The wave amplitude is a = $H_{br}/2$. The linear dispersion relation yields the wave number

$$k = \frac{1}{g}\left(\frac{2\pi}{T_{br}}\right)^2$$

and ak defines the *local wave steepness*. However, if shorter waves are riding on longer waves this method splits the underlying long wave and yields unrealistically large steepness values, as it underestimates T_{br} (Figure 1b). To rectify this bias, *Banner et al.* (2002) applied a riding wave removal scheme which progressively detects and removes riding waves through iterative processing starting with the highest frequency resolved. The occurrence and characteristic dimensions of riding waves are retained in a file and a wave is then removed from the elevation series by replacing it with a cubic polynomial spliced to the underlying longer wave form. Subsequently, the association between breaking events and recorded waves is based on minimizing the relative lag between the time of the breaking event and the time of the nearest local crest, while also satisfying a local steepness threshold.

(ii) Hilbert analysis: The Hilbert transform of a signal $X(t)$ is defined as:

$$H(t) = \frac{1}{\pi} P \int_{-\infty}^{\infty} \frac{X(t')}{(t - t')} dt' \qquad (1)$$

Due to a possible singularity at $t = t'$, the integral has to be taken as a Cauchy principal value P. The Hilbert transform defines the local amplitude

$$a_{loc} = \left(X^2(t) + H^2(t)\right)^{1/2}, \qquad (2)$$

and frequency

$$\omega_{loc} = \phi_t, \qquad (3)$$

where $\phi = \tan^{-1}\left(H(t)/X(t)\right)$. (Note, if $X(t) = \cos(\omega t)$ it follows $H(t) = \sin(\omega t)$ and $\phi(t) = \omega t$). However, the classical Hilbert analysis is most meaningful for narrow-banded signals. Broad-banded signals, like surface elevation records, have to be divided into a finite number of *intrinsic mode functions* (IMF), by way of the *empirical mode decomposition* (EMD), before the Hilbert analysis can be applied (*Huang et al*., 1998). An IMF is defined as a function fulfilling the condition that the number of zero-crossings and the number of local maxima differ by not more than one. The IMFs are generated in an iterative way as the difference between the signal and the mean of a spline fitting through all local maxima and a spline fitting through all local minima. This sifting process is repeated until the IMF conditions are met. The so obtained IMF is subtracted from the time series and the iteration continues with the residual signal until only a monotonic signal remains. Typically, surface height records yield decomposition into $N = O(10)$ IMFs. Then, the surface elevation time series may be represented as a Hilbert expansion

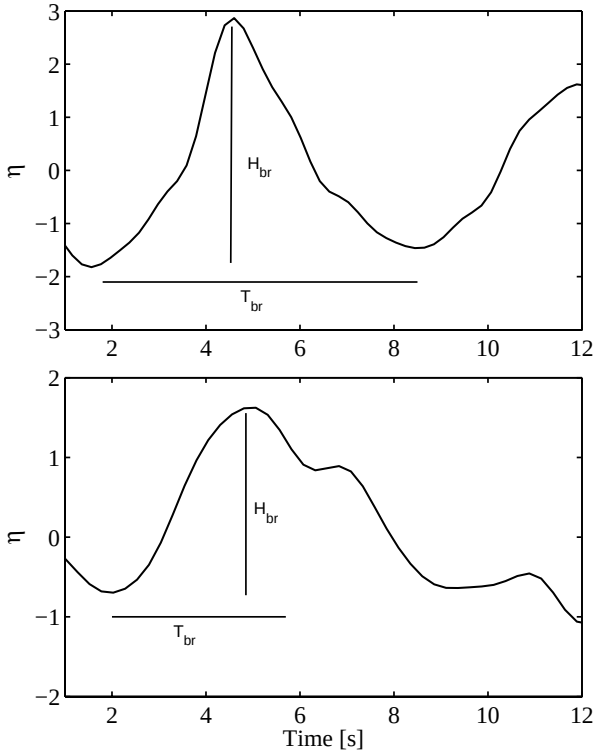

Figure 1. Surface elevation time series illustrating individual wave definition by zero-crossing analysis. H_{br}, T_{br} are the height and period of the detected individual wave. a) No riding wave. b) A riding wave splits the underlying long wave.

$$\eta(t) = \sum_{j=1}^{N} a_j(t) \exp\left(i\phi_j(t)\right), \quad (4)$$

where $a_j(t)$, $\phi_j(t)$, $\omega_j(t) = d\phi_j / dt$ are amplitude, phase and frequency of the IMFs, respectively. The instantaneous amplitude of the signal is

$$A(t) = \sum_{j=1}^{N} a_j(t) \quad (5)$$

and the instantaneous frequency is $\omega_k(t)$, where *k* corresponds to the dominant IMF at time *t*: $a_k(t) = \max(a_j(t), j = 1...N)$. Thus, $A\omega_k^2 / g$ defines the *steepness of the instantaneous dominant wave*. Note that we chose the total amplitude *A(t)* rather than the amplitude of the dominant IMF $a_k(t)$. At a single point all IMFs contribute to the surface height but the dominant wavelength is not affected by high frequency IMFs. However, at the crest location of locally dominant waves the difference between *A(t)* and $a_k(t)$ is not very significant.

(iii) Wavelet analysis: The analysis seeks segments of the time series which resemble a short, predefined wavelet. By choosing a suitable form of the wavelet, small wave groups are detected and the associated wave steepness may be calculated. The wavelet transform of a signal $X(t)$ is

$$W(p,q) = |p|^{-1/2} \int X(t) \psi\left(\frac{t-q}{p}\right) dt, \quad (6)$$

where the function $\psi(\xi)$ is the wavelet. Particularly well suited for wave slope analysis is the Morlet wavelet

$$\psi(\xi) = \exp(-iK_0 q / p) \exp\left(-(q/p)^2 / 2\right) \quad (7)$$

where the constant K_0 determines the number of oscillation of the wavelet. In the case of the Morlet wavelet, the local peak, at a given q_0, of the wavelet transform $W(p_0, q_0)$, where p_0 represent the scale of the wave and q_0 the location of the wave crest, is directly proportional to the *average steepness of the group* detected by the wavelet transform $(ak)_{wl} = CW(p_0, q_0)$. The proportionality factor C has to be determined from the wavelet analysis of simple known sinusoid test cases (*Scott et al.*, 2005).

Dynamic breaking criterion

The dynamic wave breaking criterion is the most amenable to oceanic observations. In fact, the primary measurement of wave rider buoys is acceleration and only its double integration yields the surface elevation. Thus, in principle, wave riders may be used to detect wave breaking. Major limitations are the crest avoidance of the buoy and sensor tilt which results in a reduction of the gravitational acceleration along the sensor axis and therefore an apparent upward acceleration. Also, there is uncertainty about the acceleration threshold associated with wave breaking. Some observations give *g*/2 as expected (*e.g. Snyder et al.*, 1983) but other observations show wave breaking at accelerations less than *g*/2 (*e.g. Holthujsen and Herbers*, 1986).

Indirect breaking criteria

A fourth class of wave breaking definitions is based on the post-breaking signature, most commonly the visual signal of air entrainment (whitecapping) (*e.g. Melville and Matusov*, 2002). Somewhat more objective measurements, but dependent on an unknown threshold, are sub-surface conductivity changes (*Gemmrich and Farmer*, 1999) or underwater sound (*Ding and Farmer,* 1994). Microscale breakers do not entrain air but may be detected, with infrared imagers, as surface skin disruption (*e.g., Jessup*, *et al.*, 1997).

Wave breaking probability

Traditionally, the frequency of wave breaking $\tilde{P}_{brk}$ has been defined as the total number of breaking crests passing a fixed point per unit time. Alternatively, the breaking probability per dominant wave is:

$$P_{brk} = 2\pi \frac{\tilde{P}_{brk}}{\omega_p}, \quad (8)$$

where ω_p is the dominant wave frequency. At first glance, the breaking frequency correlates with wind speed (more frequent breaking at increased wind speed) and to a somewhat lesser extend with wave age (reduction in wave breaking as the wave age increases). However, at best these correlations hold for individual storm events and different observations at similar wind speed or wave age report vastly different breaking probabilities. For a short review see *Gemmrich and Farmer* (1999) where the authors also report a significant positive correlation between breaking probability and the energy input from the atmosphere into the wave field, normalized by the wind energy input into a developed sea.

It is well known even to the casual observer that wave breaking occurs at a wide range of scales. This breaking scale is of great importance to all physical processes as-

sociated with wave breaking. For example, a small scale breaker dissipates less energy than a breaking dominant wave. Therefore, we are interested in breaking probabilities of different wave scales,

$$P(c) = \frac{N_{brk}(c, c+\Delta c)}{N_{all}(c, c+\Delta c)}, \quad (9)$$

where N_{brk} is the number of *breaking wave crests* propagating with velocities in the range $(c,c+\Delta c)$ passing a fixed point and N_{all} is the total number of *wave crests* propagating with velocities in the range $(c,c+\Delta c)$ passing a fixed point. *Banner et al.* (2002) found $P(c)$ to correlate well with the local wave saturation

$$\sigma_f(\omega) = \omega^5 S(\omega)/(2g^2), \quad (10)$$

where $S(\omega)$ is the power spectrum of the surface elevation. The breaking probability increased roughly linearly with wave saturation.

Given the slope spectrum $\int k^2 S(\omega) d\omega$, it readily follows that the mean wave slope ms within the fractional bandwidth $d\ln(\omega) = d\omega/\omega$ is a function of the wave saturation:

$$ms = \frac{1}{g}\left(\int_{\ln(\omega_1)}^{\ln(\omega_2)} \omega^5 S(\omega)\, d\ln(\omega) \right)^{1/2} \quad (11)$$

Thus, the wave saturation is a measure of the wave steepness within a spectral band, reflecting the nonlinearity of the waves. Normalization of the wave saturation by the directional spreading of the wave spectrum revealed a common normalized saturation threshold for the onset of wave breaking at all wave scales examined (in the range $\omega_p \le \omega \le 2.5\ \omega_p$). This suggests that the wave breaking probability of dominant as well as the wave breaking probability of shorter waves is associated primarily with a threshold behavior linked to the nonlinear wave group hydrodynamics.

Multiscale breaking rate

Defining multiscale breaking probabilities by equation (1) requires the knowledge of the total number N_{all} of wave crests of a certain scale passing a fixed point. However, this measurement is commonly not available. A more practical measure was introduced by *Phillips* (1985). Realizing that the scale of a breaking wave may be defined by the length of the breaking crest and its propagation speed, he defined $\Lambda(c)$, the spectral density of breaking wave crest length per unit area and velocities in the range $(c,c+\Delta c)$. So far, observations of $\Lambda(c)$ are limited (*Phillips et al.*, 2001; *Melville and Matusov,* 2002).

Inherent in any multiscale breaking analysis is the basic assumption that wave breaking is a narrow-banded process. Contingent on that assumption, the passage rate of breaking crests propagating at speed c past a fixed point is $c\Lambda(c)$. As breaking crests propagate they turn over a fraction of the sea surface. The fractional surface turnover rate per unit time is

$$R = \int c\Lambda(c) dc \quad (12)$$

which can also be interpreted as the breaking frequency at a fixed point $\tilde{P}_{brk} = R$ (*Phillips,* 1985).

Of further relevance of the quantity $\Lambda(c)$ is the fact that its fourth and fifth moment can be related to the dynamics of wave breaking. Towed hydrofoil experiments (*Duncan,* 1981) established the rate of energy loss per unit length of breaking crest to be proportional to c^5, where c is the crest propagation speed. Therefore, the wave energy dissipation due to the breaking of waves of scale corresponding to phase speed c is

$$\varepsilon(c)\, dc = b\rho g^{-1} c^5 \Lambda(c)\, dc \quad (13)$$

where b is an unknown, nondimensional proportionality factor, assumed to be constant (*Phillips,* 1985). The total energy dissipation is

$$E = b\rho g^{-1} \int c^5 \Lambda(c) dc \quad (14)$$

and the momentum flux from the waves to currents

$$M = b\rho g^{-1} \int c^4 \Lambda(c) dc\,. \quad (15)$$

Observations

The FAIRS (Fluxes, Air-Sea Interaction and Remote Sensing) experiment took place in September-October 2000, roughly 150 km off Monterey, California from aboard the research platform FLIP. Two downward looking black and white video cameras were mounted on the starboard boom to supplement subsurface turbulence measurements (*Gemmrich and Farmer,* 2004). The video recordings were digitized and whitecap information, in particular $\Lambda(c)$, extracted. The video footprints of roughly 9×12 m and 15×20 m and 0.02 m resolution resolved all small- scale whitecaps but did not always capture the full breaking crest length of dominant breakers.

In our analysis, whitecap properties are based on the differences between successive video frames. This method filters out all stationary objects, including sun glitter and non-actively breaking whitecaps. The remaining objects are analyzed with the MATLAB image processing toolbox to extract the axis length and centroid of each object. Tracking the translocation of the centroid

yields the apparent breaking wave speed $\hat{c}$ as well as its propagation direction θ. Smaller breaking waves are likely advected by the orbital motion of underlying larger waves u_{orb}. This Doppler shift is removed, based on the modified dispersion relation

$$\omega_{obs} = \omega_{\text{int}} + ku_{orb} \tag{16}$$

with $u_{orb} = A\omega_k$, and the true wave propagation speed c, corresponding to the intrinsic frequency ω_{int}, is obtained. We base speed estimates c on the average propagation speed within 0.3 s of detection and length estimates on the average object length calculated from all image frames. Thus, each whitecap is assigned one speed c, one crest length Λ and one propagation direction θ. Note, this is different to the method reported by *Melville and Matusov* (2002) which is based on decomposing the boundary of each whitecap into a number of elements each of a scale of approximately 0.5 m. Using PIV they estimated the length and the velocity relative to the whitecap centroid for each element. Elements with a positive, forward relative velocity are considered to be actively breaking. All actively breaking elements entered the $\Lambda(c)$ statistics, with a single whitecap contributing to various different speeds.

Wave field information utilized in this report is based on single point acoustic range finder data, kindly provided by Dr. Jessup (APL, Seattle)

Occurrence and scale of wave breaking

Here we report on four data sets recorded under various wind forcing and wave field conditions (Figure 2). Data set 1 represents a growing sea, sets 2 and 3 nearly fully developed seas, and set 4 a growing sea in the presence of significant swell.

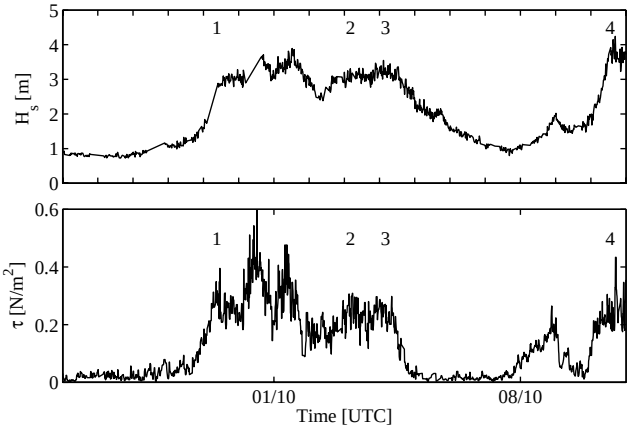

Figure 2. Significant wave height H_s (top panel) and wind stress τ during FAIRS. Numbers 1-4 indicate the timing of the data sets presented in this study.

Breaking scale

Wave breaking occurs over a wide range of scales (Figure 3). However, the breaking scales cover different ranges of the wave spectrum, depending on wave development. In the young sea case, phase speeds of breaking waves span from approximately 1/10 of the dominant phase speed (*i.e.* with a wavelength corresponding to 1/100 of the dominant wavelength) up to the dominant waves. On the other end, in a fully developed sea we observed hardly any breaking at scales corresponding to phase speeds larger than about c_p. As the wave age increases the distribution of breaking scales narrows significantly and the peak of the breaker phase speed distribution shifts from about $0.4c_p$ to $0.2c_p$.

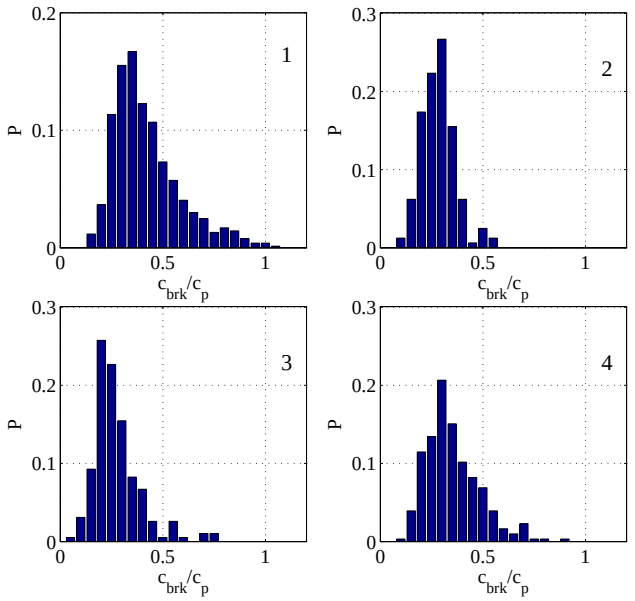

Figure 3. Distributions of the scale of breaking waves c_{brk}/c_p for four data sets indicated in Fig. 2; c_{brk} ,c_p are the phase speeds of breaking waves and dominant waves, respectively.

In terms of directional distribution we do not see any significant differences between the four data sets. The Gaussian distributions center around the mean wind direction and have a standard deviation of approximately 30º (not shown).

Generally, the breaking crest length of individual events increases with wave scale. Therefore, the total breaking crest length per unit area and propagation speed, $\Lambda(c)$, shows a slightly different behaviour than the breaking occurrence rates given in Figure 3. For all four data segments, $\Lambda(c)$ peaks at intermediate wave scales corresponding to $c/c_p \approx 0.3$ (Figure 4).

Phillips' (1985) concept of a spectral equilibrium range assumes for intermediate wave scales a balance

between energy input, non-linear energy transfer and energy dissipation. In this equilibrium range the wave height spectrum scales as

$$S(\omega) \propto \omega^{-4}. \quad (17)$$

Therefore, the form of the energy input

$$E_{in}(\omega) = g\beta S(\omega) \quad (18)$$

and the wave growth factor

$$\beta \propto \omega(u_w / c)^2 \text{ (Plant, 1982)}, \quad (19)$$

where u_w is some measure of the wind speed, translates into a c^{-1} dependence of the spectral wind energy input in c-space, $E_{in}(c) \propto c^{-1}$. The equilibrium concept requires the same c-dependence of the spectral dissipation and therefore, based on (13), it follows that $\Lambda(c) \propto c^{-6}$.

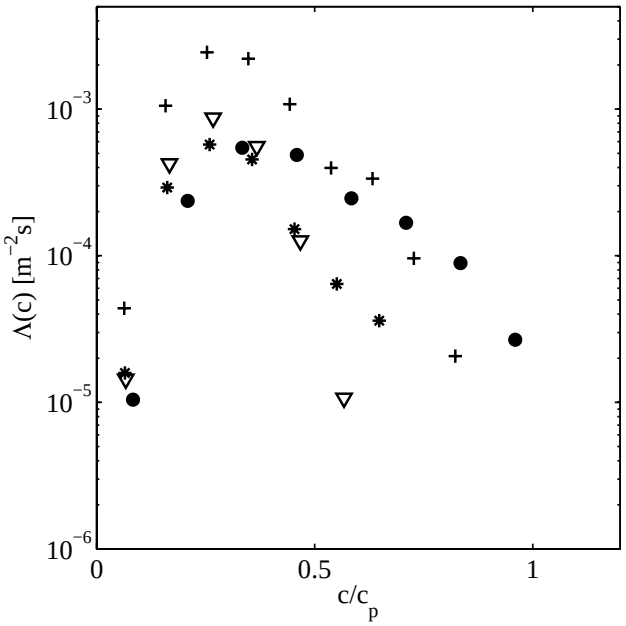

Figure 4. Breaking crest length as function of normalized crest propagation speed c/c_p, i.e. the normalized phase speed of breaking waves. The symbols (•,▽,*,+) correspond to data sets (1,2,3,4), respectively.

At scales larger than the peak of the observed $\Lambda(c)$ distribution, $\Lambda(c)$ indeed falls off approximately as c^{-6}, consistent with the equilibrium range concept. (Although this does not show clearly in Figure 4 it is seen in a graph of $\Lambda(c)$ versus c as will be described in a forthcoming paper). However, according to (13) the low $\Lambda(c)$ values at small scales imply reduced dissipation, and thus the equilibrium concept requires reduced energy input and/or increased non-linear transport to larger wave scales compared to the current formulation of spectral wave models. It should be noted that the inferences made about the slope of $\Lambda(c)$ are based on the assumption that the proportionality factor b in (13) is scale independent, as found in the somewhat unrelated hydrofoil experiment by *Duncan* (1981). Moreover, the value of b is very uncertain with reported values applicable to the ocean ranging from $b \approx 10^{-4}$ (*Phillips et al.,* 2001) to $b \approx 10^{-2}$ (*Melville and Matusov*, 2002) and assumed to be scale independent.

Total breaking rate

The overall breaking rate R, given by (12), is equivalent to the fractional surface area turnover rate, and thus an important quantity for air-sea exchange processes. It also provides insight to what conditions are favourable to wave breaking. *Banner et al.* (2002) found the breaking rate at specific scales to depend on some measure of the mean steepness. Here we explore possible correlations between the total breaking rate and wave steepness.

In this context it is interesting to note that in wave tank experiments the wave groupiness, believed to play an important role in the generation of rogue waves, also determines the limiting steepness $(ak)_{\max}$ of these extreme waves (*Wu and Yao,* 2004). Assuming that larger wave amplitudes, i.e. steeper waves, are prevented due to wave breaking implies that the steepness threshold of the geometric wave breaking criterion is equal to $(ak)_{\max}$.

Wu and Yao (2004) report a very strong inverse dependence of the maximum attainable wave steepness $(ak)_{\max}$ on the non-dimensional wave group bandwidth

$$\nu = \sqrt{\frac{m_2 m_0}{m_1^2} - 1} \quad (20)$$

where $m_i = \int_{1/2\omega_p}^{3/2\omega_p} \omega^i S(\omega) d\omega$ is the i$^{\text{th}}$ moment of the power spectrum S(ω) (*Longuet-Higgins*, 1984). For long groups ($\nu \to 0$, i.e. narrow peaked spectrum) $(ak)_{\max}$ is close to the Stokes limit π/7, whereas for $\nu = 0.2$ (shorter groups, broader spectrum) the authors found a sharply reduced value $(ak)_{\max} \simeq 0.2$.

If wave breaking is the limiting process, one would expect that in cases of small $(ak)_{\max}$ wave breaking is more frequent than in cases with a larger limiting steepness, yielding a positive correlation between wave breaking and bandwidth. No well defined relation between breaking rate and bandwidth emerges from our data, which might, however, partially be due to the lim-

ited range of bandwidth in our observations (Figure 5a). It is very likely that processes associated with the directional wave field (e.g. directional focusing) are important for wave breaking and the excellent correlation between $(ak)_{\max}$ and ν observed in the controlled 2-dimensional wave tank environment might also not be as strong under open ocean conditions.

The fact that the limiting steepness $(ak)_{\max}$ of extreme waves varies widely also suggests that the critical wave steepness that will lead to wave breaking does not have a fixed value. Nevertheless, one expects a wave field with a significant fraction of 'steep' waves to exhibit more breaking than a wave field with fewer 'steep' waves. To test this assumption we calculate the steepness $A\omega_k^2/g$ for each individual wave crest and determine the fraction P of wave crests with steepness above a given threshold. The breaking rate increases approximately linearly with the fraction of steep waves (Figure 5b). It turns out that this scaling is not very sensitive to the threshold steepness values if chosen in the range 0.3 – 0.45, though absolute values of P change.

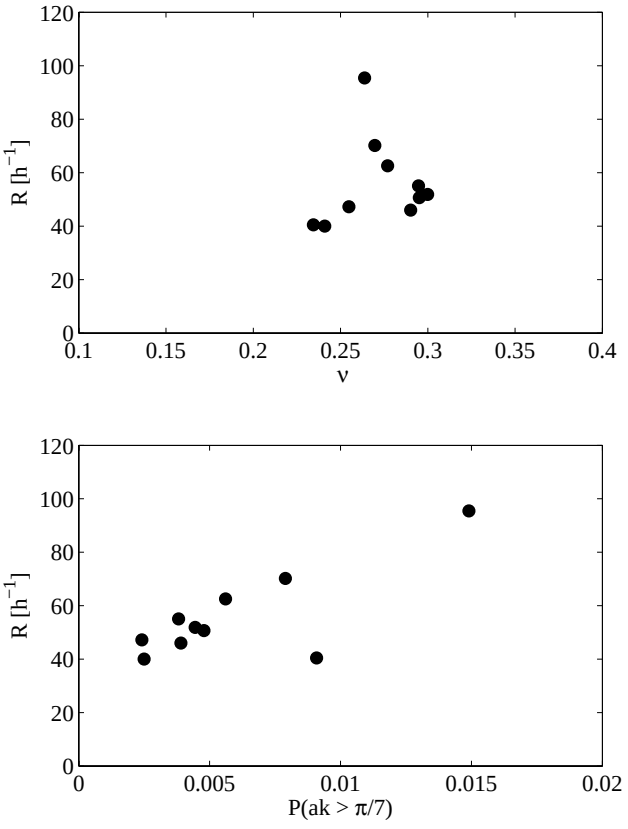

Figure 5. Breaking rate R (equation 12) versus nondimensional bandwidth ν (equation 20) (top) and fraction of wave crests with wave steepness larger than π/7 (bottom).

Conclusions

Wave breaking criteria based on geometric, kinematic or dynamic properties of individual waves are not easily applicable to oceanic observations, mainly due to uncertainties in identifying individual waves and unknown threshold values. Most accessible is the post-breaking criterion of whitecap generation. *Phillips* (1985) equilibrium range theory includes a statistical description of wave breaking, its kinematics and dynamics. The required key quantity $\Lambda(c)$, where $\Lambda(c)dc$ is the length of breaking crests per unit area propagating with speeds in the range $(c, c+dc)$, may be extracted from video imagery of the sea surface. $\Lambda(c)$ peaks at intermediate wave scales and for larger scale it is approximately proportional to c^{-6} which is consistent with the current form of spectral wave models. However, the steep decline of $\Lambda(c)$ at small scales implies reduced energy input and/or more rapid non-linear transfer in order to satisfy the equilibrium assumption. However, the uncertainty in the proportionality factor b, relating the breaking crest length to energy dissipation, further complicates this issue. Independent co-located measurements of energy dissipation and breaking crest lengths $\Lambda(c)$ are required to determine whether the proportionality factor b is indeed independent of c.

In a young wave field, breaking that generates whitecaps occurs at a wide range of scales corresponding to breaking wave phase speeds from about 0.1 – 1.0 c_p. The most frequent breakers occur at scales corresponding to $c_{brk} \approx 0.4\ c_p$. In developed seas the distribution of breaker speeds narrows, with almost all breaking wave speeds $c_{brk} < 0.5\ c_p$, and the peak of the distribution shifts to 0.2 c_p.

As wave breaking is the main limiting factor of wave growth, the breaker scale distribution is also expected to impact processes like rogue wave generation. Breaking of waves close to the dominant wave scales would severely limit the generation of rogue waves. Thus, the lack of breaking of large scale waves in older seas implies a much greater likelihood of rogue wave occurrence in developed seas than in young seas.

In wave tanks the wave-group bandwidth seems to be a very good indicator of limiting extreme wave steepness, with reduced attainable steepness as the wave spectral bandwidth increases (*Wu and Yao,* 2004). It is not entirely clear whether the limiting extreme wave steepness is equivalent to the critical steepness that leads to breaking. If this was the case, the breaking rate would be a strong increasing function of wave spectral bandwidth, which is not supported in our open ocean data set. Since

rogue wave generation is mainly linked to large scale waves, a better correlation might be expected between bandwidth and the breaking rate of larger scale waves. Unfortunately, our data sample of dominant wave breaking is too limited to allow for meaningful statistics.

On the other hand, the total breaking rate of all scales is clearly related to the fraction of waves exceeding a certain steepness threshold. This result is nearly independent of the steepness threshold, if chosen in the range $0.3 < ak < 0.45$.

Most records of rogue waves under natural conditions do not include any information on the occurrence and strength of their breaking. Therefore, it is not known whether wave breaking indeed limits the actual extreme wave. The following two limiting rationales exist: (i) Rogue waves grow until wave breaking cuts off any further increase in height. For example, this situation occurs when waves propagate into a strong divergent surface current. (ii) On the other hand, a rogue wave generated by some kind of focusing mechanism might not actually reach the point of breaking with its height being limited by the conditions of the underlying focusing wave trains.

Our results indicate that wave breaking affects the overall wave field, and therefore at least indirectly the probability of rogue wave generation. A systematic study of rogue wave steepness and spectral wave bandwidth could shed some light on the question if the height of extreme waves is limited by wave breaking or by the generation mechanisms. This is also important from a practical point of view as a breaking rogue wave could potentially cause more damage than a non-breaking wave of the same dimension.

Acknowledgments. I thank Mike Banner and Chris Garrett for the frequent discussions that contributed significantly to this work. I also thank the organizers of the 'Aha Huliko'a workshop for the opportunity to participate in this stimulating workshop. Andy Jessup kindly provided the surface elevation time series. Funding by the Canadian Foundation of Climate and Atmospheric Sciences (CFCAS) is gratefully acknowledged.

References

Ardhuin, F., A. D. Jenkins, D. Hauser, A. Reniers and B. Chapron, Waves and operational oceanography: toward a coherent description of the upper ocean, *EOS., 86(4)*, 37, 40, 2005.

Banner, M. L., J. R. Gemmrich and D. M. Farmer, Multiscale measurements of ocean wave breaking probability, *J. Phys. Oceanogr., 32,* 3364 – 3375, 2002.

Ding, L. and D. M. Farmer, Observations of breaking surface wave statistics, *J. Phys. Oceanogr*. *24*, 1368-1387, 1994.

Duncan, J. D., An experimental investigation of breaking waves produced by an airfoil, *Proc. R. Soc, Lond. A*, *377*, 331-348, 1981.

Gemmrich, J. R. and D. M. Farmer, Near-surface turbulence in the presence of breaking waves, *J. Phys. Oceanogr*., *34*, 1067-1086, 2004.

Gemmrich, J. R. and D. M. Farmer, Observations of the scale and occurrence of breaking surface waves, *J. Phys. Oceanogr*., *29*, 2595-2606, 1999.

Holthuijsen, L. H., and T. H. C. Herbers, Statistics of breaking waves observed as whitecaps in the open sea, *J. Phys. Oceanogr., 16,* 290-297, 1986.

Huang, N. E., Z. Shen, S. R. Long, M. C. Wu, Q. Zheng, N.-C. Yen, C. C. Tung & H. H. Liu, The empirical mode decomposition and the Hilbert spectrum for nonlinear and non-stationary time series analysis. *Proc. R. Soc, Lond. A*, 454, 903-955, 1998.

Jessup, A. T., C. J. Zappa, M. R. Loewen and V. Heasy, Infrared remote sensing of breaking waves, *Nature, 385,*52-55, 1997.

Longuet-Higgins, M. S., Accelerations in steep gravity waves, *J. Phys. Oceanogr., 15,* 1570–1579, 1985

Longuet-Higgins, M. S., Statistical properties of wave groups in a random sea state, *Philos. Trans. R. Soc. London, Ser. A, 312,* 219-250, 1984.

Melville, W. K. and P. Matusov, Distribution of breaking waves at the ocean surface. *Nature, 417,* 58-63, 2002.

Phillips, O. M., F. L. Posner and J. P. Hansen, High range resolution radar measurements of the speed distribution of breaking events in wind-generated ocean waves: Surface impulse and wave energy dissipation rates, *J. Phys. Oceanogr., 31*, 450-460, 2001.

Phillips, O. M., Spectral and statistical properties of the equilibrium range in wind-generated gravity waves, *J. Fluid Mech*., 156, *505-531,* 1985.

Plant, W. J., A relantionship between wind stress and wave slope. *J. Geophys. Res., 87*, 1961-1967, 1982.

Scott, N. V., T. Hara, E .J. Walsh and P. A. Hwang, Observations of steep wave statistics in open ocean waters, *J. Atmos. Ocean. Tech., 22*, in press, 2005.

Snyder, R., L. Smith, and R. Kennedy, On the formation of whitecaps by a threshold mechanism. Part III: Field experiment and comparison with theory. *J. Phys. Oceanogr., 13,* 1505–1518, 1983

Wu, C. H. and A. Yao, Laboratory measurements of limiting freak waves on currents, *J. Geophys. Res., 109*, C12002, doi:10.1029/2004JC002612, 2004.